Detailed Microvariational RRKM Master Equation Analysis of the Product Distribution of the $C_2H_2 + CH(X^2\Pi)$ Reaction over Extended Temperature and Pressure Ranges

Luc Vereecken and Jozef Peeters*

Department of Chemistry, University of Leuven, Celestijnenlaan 200F, B-3001 Leuven, Belgium

Received: March 1, 1999; In Final Form: May 12, 1999

We present a detailed microvariational RRKM Master Equation analysis of the $CH(X^2\Pi) + C_2H_2$ reaction products distribution, based on an earlier quantum chemical characterization of the accessible potential energy surface. This is the first time that the pressure and temperature dependence of the product distribution has been analyzed and discussed. Also, an extensive error analysis is performed, aiming to quantify the confidence region for the predicted product distribution as a function of temperature and pressure. The results indicate that for pressures up to several atmospheres, H + triplet prop-2-enylidene (HCCCH) and H + singlet cyclopropenylidene (cyc-C_3H_2) are the main reaction products, with smaller contributions from $C_3H + H_2$ formation. Typical net yields are 90% HCCCH, 7% cyc-C_3H_2 at 300 K and 82% HCCCH, 11% cyc-C_3H_2 at 2000 K, for pressures from 0 to 5 atm. Substantial stabilization of 2-propynyl radicals (H_2CCCH) occurs only at higher pressures in excess of 10 atm of air. Our results disagree with another recent theoretical study, which did not consider several of the most important entrance and exit channels.

Introduction

The reaction of methylidyne radicals with acetylene, $CH(X^2\Pi) + C_2H_2$, plays an important role in many chemical reaction mechanisms, such as the formation of PAH and soot precursors in hydrocarbon combustion[1−4] and the formation of small hydrocarbons in the interstellar medium.[5,6] The overall rate constant of the $CH + C_2H_2$ reaction has been measured experimentally (see Table 1) for pressures up to 400 Torr, at temperatures ranging from 170 to 700 K. The results indicate that this reaction is very fast indeed, with a rate constant approaching the collision limit. Unfortunately, little is known of the temperature- and pressure-dependent product distribution[7] of this reaction:

$$\begin{aligned} CH(X^2\Pi) + C_2H_2 \rightarrow C_3H_3^{\dagger} &\xrightarrow{M} C_3H_3 \\ &\rightarrow C_3H_2 + H \\ &\rightarrow C_3H + H_2 \end{aligned}$$

The reaction of CH with C_2H_2 forms initially chemically activated C_3H_3 intermediates, which can undergo isomerization reactions until they dissociate to $C_3H_2 + H$ or $C_3H + H_2$ or redissociate to the initial reactants $CH + C_2H_2$. These unimolecular reactions occur in competition with energy loss processes in collisions with the bath gas M, which can lead to thermalized C_3H_3 radicals. Direct experimental measurement of the product distribution is hampered by the large number of possible isomers of the C_3H_x intermediates and reaction products and by the wide range of reaction conditions in which this reaction plays a role, extending from the very cold, near-zero pressure conditions in the interstellar medium to the high-temperature and high-pressure conditions in internal combustion engines.

In this paper, we present the results of a microvariational RRKM study of the product distribution of the $CH(X^2\Pi) + C_2H_2$ reaction based on our earlier detailed DFT and CASPT2 characterization of the potential energy surface;[8] temperatures from 100 to 3000 K are considered, with pressures ranging from 10^1 to 10^9 Pa of air (10^{-4}−10^4 atm). The sensitivity of the obtained results to the most important parameters in the kinetic model is analyzed, providing an estimate of the expected error as a function of temperature and pressure. Where possible, our results will be compared to the available experimental data; a discussion of the recent RRKM study by Guadagnini and co-workers[9] is also included. The primary focus of this work will be on providing information on the product distribution and the dependence thereof on temperature and pressure, rather than on the overall rate constant which has already been well-established experimentally. The time scale for reaction of the *activated* C_3H_3 radicals as formed in the $C_2H_2 + CH$ reaction is very short, on the order of nanoseconds, and is therefore little perturbed by secondary reactions with other species present in the reaction mixture. The concentration and fate of the *stabilized* C_3H_3 radicals (and the other reaction products), on the other hand, depends on the physical system under consideration: because of the deep energy wells, thermal isomerization or dissociation can readily be outrun by bimolecular reactions with other species present. The large difference in time scale between the activated C_3H_3 reactions versus bimolecular and thermal C_3H_3 reactions allows us to separate in good approximation the

TABLE 1: Experimental Values for the Rate Constants for the Reaction of CH with Acetylene

reference	T (K)	P (Torr)	k (10^{-10} cm^3 molec^{-1} s^{-1})
Bosnali and Perner[23] (1971)	298		0.75
Butler et al.[24] (1981)	298	100	2.2
Berman et al.[25] (1982)	171	100	5.3
	657	100	4.1
Thiesemann et al.[22] (1997)	291	100	3.1
	288	400	2.9
	475	100	3.0
	588	100	2.9
	710	100	2.6

* Corresponding author. E-mail: Jozef.Peeters@chem.kuleuven.ac.be.

10.1021/jp990720w CCC: $18.00
Published on Web 06/25/1999

immediate product distribution of the C_2H_2 + CH reaction from the long-term evolution of the concentrations of the reaction products. Experimentally observable concentrations of the intermediates and products can then be predicted by kinetic modeling on the reaction mixture.

General Computational Method

The temperature- and pressure-dependent product distribution of the C_2H_2 + CH($^2\Pi$) reaction was obtained by Master Equation analysis in steady-state conditions. All calculations were performed using our general purpose URESAM[10] kinetics computer program suite, capable of describing the formation of adduct(s) in a (number of) initial reaction(s), followed by any complex system of unimolecular isomerization and (re)-dissociation reactions, competing with energy transfer processes. The solution methods, using an energy grained Master Equation, are based on a stochastic description of the kinetic problem; for the steady-state solutions of the Master Equation for the C_2H_2 + CH system, we mainly used the CSSPI[10] method implemented in URESAM. In this method, the reactions of the C_3H_3 intermediates are viewed as a stochastic random walk through the species-energy space, which can be described as a continuous time Markov chain. The reaction rate of the initial reaction is explicitly balanced with the rate of product formation, be it dissociation or stabilization into a sink, ensuring steady-state conditions. This allows the computational problem to be expressed as a set of linear equations, which can be solved directly. The method yields the steady-state population of the intermediates; these can be transformed to the product distribution by calculating the weighted average over the energy-specific rate constants $k(E)$ for dissociation or stabilization. For a number of reaction conditions, the CSSPI results were verified against DCPD[10] calculations. This method allows for a direct calculation of the product distribution by describing the stochastic random walk as a discrete time Markov chain. This leads to a quite different computational problem, requiring the calculation of the infinite power of the one-step transition matrix, but should yield the same product distribution. The degree of agreement of the DCPD and CSSPI results will provide an indication of the numerical stability of these methods.

The energy specific rate constants $k(E)$ for the unimolecular reaction steps in the system that proceed through saddle-point transition states are calculated by standard RRKM theory[11−14]:

$$k(E) = \frac{\alpha G^{\ddagger}(E - E_0)}{hN(E)}$$

where the harmonic density of states $N(E)$ for the reacting molecule and the sum of accessible states $G^{\ddagger}(E - E_0)$ for the transition state are calculated by direct count using the Beyer−Swinehart[15,16] algorithm, based on the quantum chemical characterization[8] of the potential energy surface (vide infra). The reaction path degeneracy α is calculated as the ratio $\sigma/\sigma^{\ddagger}$ of the rotational symmetry number of the reactant, σ, and transition state, $\sigma^{\ddagger}$. To more accurately describe the *barrierless* dissociation reactions, e.g., $C_3H_3 \rightarrow C_3H_2 + H$ and $C_3H_3 \rightarrow C_2H_2 + CH$, we implemented microvariational RRKM theory. The reaction path leading from the C_3H_3 adduct to the dissociation products is described in detail by calculating the relative energies and rovibrational characteristics for successive geometries along the reaction coordinate, and, for each given energy, the bottleneck structure with the minimum number of accessible internal quantum states is then located. To this end, the reaction path was established by fixing each time one geometric variable and reoptimizing all other geometric parameters; the C−H bond length was fixed when calculating the dissociation to C_3H_2 + H, and the perpendicular distance of the CH carbon to the acetylene axis was fixed for the dissociation to C_2H_2 + CH. For each RC geometry, the vibrational wavenumbers are also calculated. Interpolation of the relative energies and vibrational wavenumbers is done by means of a cubic C-spline, ensuring a smooth and natural connection through the calculated points. During this interpolation, the wavenumbers are ordered so as to obey the noncrossing rule for vibrational modes with the same symmetry. Using the resulting continuous description of the relative energy and vibrational wavenumbers along the reaction path, the sum of accessible states $G^{\ddagger}(E - E_0)$ is minimized separately for every considered excess energy E; the point on the reaction coordinate where this minimum is found should be a good approximation to the true transition state for the barrierless reaction at that energy E and provide a good basis for calculating the energy-dependent rate constant $k(E)$. In general, the position along the reaction coordinate with the lowest sum of states $G^{\ddagger}(E - E_0)$ shifts to shorter bond lengths with increasing internal energy. This can be illustrated using the results for the barrierless entrance transition states, where it was found that the C−C distance in the bottleneck structure shifts from nearly 4 Å to less than 2.5 Å when the excess energy increases from 0 to 30 kcal/mol. The microvariational approach used here captures the main features of the microvariational transition state principle for barrierless reactions; to the best of our knowledge, this is the first time that a microvariational treatment of this level is implemented in a general purpose theoretical kinetics computer program (URESAM[10]) and applied in a Master Equation analysis of a highly complex reaction mechanism. More sophisticated microvariational methods have been developed (see, e.g., refs 17−20) with a more involved treatment of the reaction coordinate or the anharmonicities of the transitional degrees of freedom; however, the quantum chemical computational demands for our approach are already so high that increasing the level of treatment at this time becomes impractical as a general tool.

The initial energy distribution function of the C_3H_3 intermediates as formed in the C_2H_2 + CH reaction is obtained from detailed balance considerations based on the RRKM formalism,[11−14] assuming thermal energy distributions for the initial reactants, CH + C_2H_2:

$$P_{\text{form}}(E)\delta E = \frac{G^{\ddagger}(E - E_0)\exp\left(-\frac{E - E_0}{kT}\right)\delta E}{\int_{E_0}^{\infty} G^{\ddagger}(E' - E_0)\exp\left(-\frac{E' - E_0}{kT}\right)\mathrm{d}E'} \quad \text{for } E \geq E_0;$$

0 otherwise

where $G^{\ddagger}(E - E_0)$ is the sum of states for the entrance transition state at the considered internal energy E. Collisional energy transfer is incorporated using Troe's biexponential model,[21] where small amounts of energy are preferentially transferred, with an exponentially decreasing probability for larger amounts of transferred energy:

$$P_{\text{transfer}}(E \rightarrow E') = \frac{1}{Q}\exp\left(\frac{E - E'}{\langle \Delta E_{\text{up}} \rangle}\right) \quad \text{for } E' > E$$

$$P_{\text{transfer}}(E \rightarrow E') = \frac{1}{Q}\exp\left(\frac{E - E'}{\langle \Delta E_{\text{down}} \rangle}\right) \quad \text{for } E' < E$$

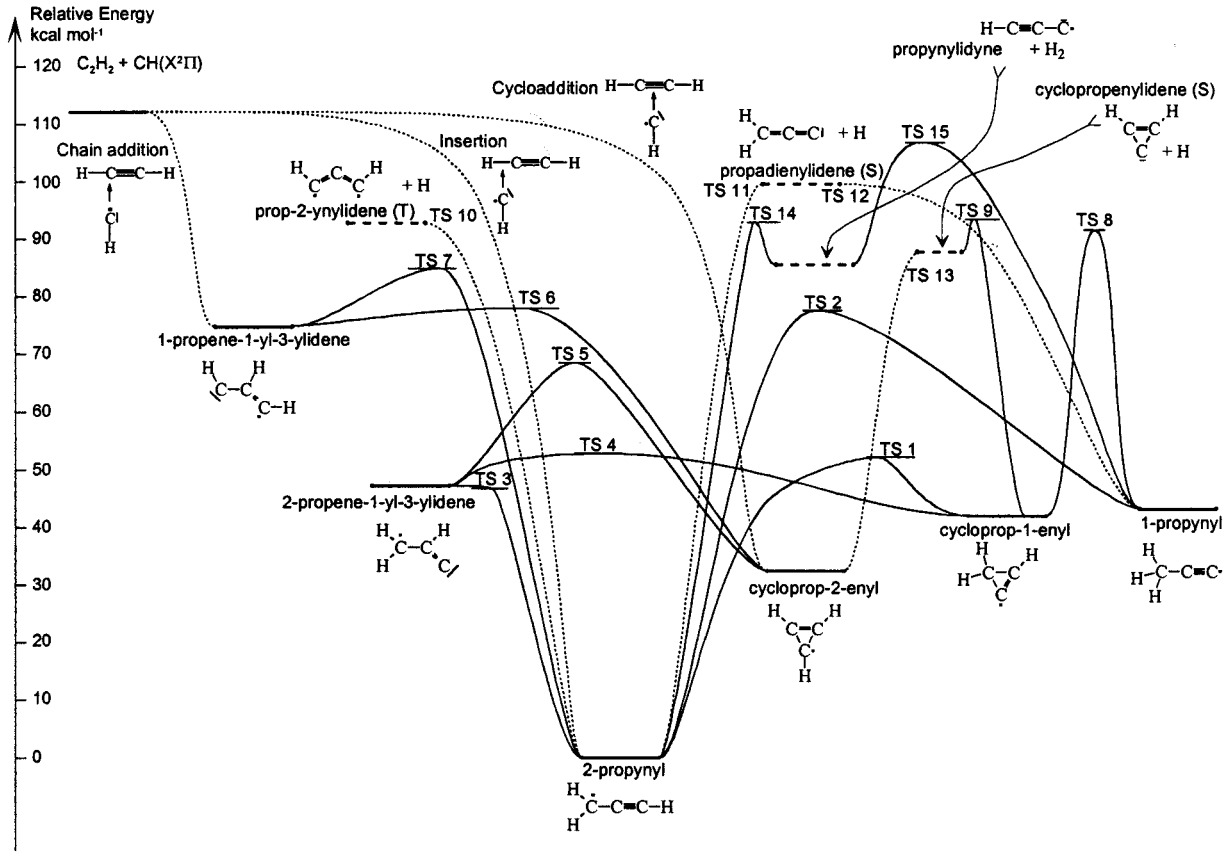

Figure 1. Schematic profile of the potential energy surface for the C_2H_2 + CH($X^2\Pi$) reaction. Solid lines represent conventional transition states; dotted lines indicate a microvariational transition state.

The parameters $\langle\Delta E_{up}\rangle$ and $\langle\Delta E_{down}\rangle$ are derived from the average transferred energy per collision $\langle\Delta E_{all}\rangle$ through detailed balancing considerations.[21] The total collision rate constant is derived from the Lennard-Jones collision frequency, where the collision integrals $\Omega^{(2,2)}$ are calculated based on the approximations given by Troe.[21] The continuous probability distributions above were all rewritten for use in a finite, grained energy space, assuming a homogeneous population within one energy grain.

Discussion of the C_3H_3 Potential Energy Surface

The potential energy surface (PES) for the C_2H_2 + CH($^2\Pi$) reaction is quite complex. We have characterized[8] it quantum chemically in great detail at the B3LYP-DFT level of theory, with verification against high-level CASPT2 calculations and literature data. Figure 1 gives a schematic representation of the PES. It was found that, in general, the DFT relative energies, vibrational wavenumbers, and rotational constants were in very good agreement with the available data. We refer to ref 8 for an extensive discussion of the PES; here we will only discuss how the data was used to formulate the kinetic model. Unless indicated otherwise, we use the DFT relative energies (including ZPE correction) and DFT vibrational wavenumbers throughout the kinetic analysis.

As a direct consequence of the dual radical/carbyne character of CH($^2\Pi$), three entrance channels can be formally distinguished for the initial reaction of CH($^2\Pi$) with C_2H_2: cycloaddition to the triple bond and insertion in the acetylene C−H bond, both barrierless carbyne reactions, and the radical chain addition on a C_2H_2 carbon atom. Obtaining these three channels proved to be the most difficult part of the characterization of the PES, mainly because of spin contamination for the (geometrically similar) insertion and chain addition channels which prevented calculation of the entire transition from reagents to adduct for these channels. It was found that, at acetylene−CH distances larger than about 3 Å (measured as $C_{C_2H_2}-C_{CH}$ distance), the three entrance channels merge into a single channel, consistent with a barrierless reaction leading into a very deep potential energy well and with no steric hindrance to make one line of approach different from another. The potential energy well for the approach of CH at those distances has an ellipsoid shape with the two acetylene carbons in the centers, as can be expected from the oblate shape of the linear acetylene itself. Calculation of the sum of states for several intermediate geometries indicates that the energy-specific transition state for low to medium excess energies is located at C−C distances larger than 3−2.5 Å, respectively, i.e., in the region where no separation of the three different entrance channels is apparent. Hence, for low to medium excess energies, the pathway obtained for the cycloaddition, which could be fully characterized, without significant spin contamination, should also be a reasonable estimate for the chain addition and insertion pathways at the relevant transition state separations. For higher excess energies, the energy-specific microvariational transition state will be located at shorter acetylene−CH distances, such that the approximation becomes worse, but these energy levels are thermally less populated, making the expected deviation not overly important. We therefore used the same pathway characteristics for all three entrance channels. Isotope substitution measurements by Thiesemann et al.[22] revealed a small (∼20%) kinetic isotope effect for deuterium substitution in the CH radical, whereas deuterium substitution in the acetylene reactant has hardly any effect. From this, the authors conclude that the acetylene C−H vibrational modes are unaffected by the incipient complex formation, but the methylidyne C−H stretch changes

slightly in the transition state. They also suggest that the use of simple loose transition state models is inadequate for describing this reaction, requiring *explicit* consideration of the changes in vibrational frequencies during capture. Our detailed characterization of the entrance transition state indeed finds that the *change* in the CH stretch vibration compared to the parent molecule is consistently 2−3 times larger than the change for the acetylene CH vibrational modes during the approach, qualitatively supporting the results of Thiesemann et al.[22]

A consequence of the merging of the three entrance channels on the PES for the considered C−C distances is that the relative importance of the entrance channels can no longer be calculated based on sum of states consideration at the transition state; selection of the adduct formed will only occur *after* the bottleneck structure has been cleared, and this selection will largely be controlled by dynamic effects, which are also a function of the (random) entering velocity, the attitude of the vector of approach, etc. To estimate the contribution for each entrance channel, we assume that the probability of formation of a certain initial adduct is proportional to the probability that the CH passes the transition state in a geometry resembling the considered adduct: approach toward the triple bond of acetylene leads to cycloaddition, toward a C−H bond leads to insertion, and toward a carbon atom results in chain addition. Since the velocity and angle of approach are random, any late changes in target adduct should largely cancel out. The fraction of the surface on an ellipsoid around the acetylene molecule and corresponding to the considered geometries then gives an estimate of the fraction of the adduct formed. The C−C−C bond angle found in TS 6 (cyclization of CHCHCH) is used to separate cycloaddition from the other two pathways; this leads to a 50% cycloaddition fraction, insensitive to the actual radius of the ellipsoid used. Separating the remaining 50% into chain addition and insertion is less obvious, but chain addition will probably be a minor pathway, since it is a radical closed-shell reaction rather than a barrierless carbyne reaction and because of the proximity of the much deeper (and therefore steeper) 2-propynyl energy well of the insertion channel. Hence, we crudely estimate that chain addition will be on the order of 10% of the total initial reaction, with 40% remaining for the insertion reaction. As discussed later, the effects of varying in the relative importance of the different entrance channels are largely attenuated by the subsequent fast isomerization reactions, making this estimate sufficiently accurate.

Six local minima were characterized, all interconnected by transition states well below the CH + C_2H_2 reactants energy level, permitting extensive isomerization. Four of the minima represent well-defined energy wells on the potential energy surface: 2-propynyl (propargyl, H_2CCCH), 1-propynyl (H_3CCC), cycloprop-2-enyl, and cycloprop-1-enyl. The most stable of these is 2-propynyl, by over 30 kcal/mol; the second most stable isomer is cycloprop-2-enyl. Besides being the two most stable isomers, these two C_3H_3 species are formed directly in the initial reaction of CH with acetylene, and they give access to the lowest energy dissociation pathways; this makes them the most crucial C_3H_3 isomers. The ground state of cycloprop-2-enyl is a structure with C_s symmetry, because of Jahn-Teller distortion, leading to three distinct wells on the PES. The barrier heights for pseudorotation, interconnecting these three minima, is only about 3−4 kcal/mol. At internal energies higher than that, as typically encountered in the present study, the rapid interconversion of the three cycloprop-2-enyl forms will cause cycloprop-2-enyl to appear as a single structure with all C−C bonds identical and three indistinguishable hydrogens. The reaction path degeneracy used in the RRKM analysis takes this into account. A second effect of this merging of the three wells is that the structure becomes looser such that the density of states can no longer be accurately calculated based on the harmonic wavenumbers of the ground state. There is at present no reliable way to calculate the resulting increase in state density, so this effect must perforce be approximated; we do this here by merely summing the densities of states of the three separate wells, even though this is almost certainly an underestimation of the true density of states, especially at high internal energies. The second cyclic isomer, cycloprop-1-enyl, has low barriers for ring breaking (TS 1 and TS 4). It will therefore readily isomerize to more stable isomers. 1-Propynyl is somewhat separated from the rest of the PES: the two pathways leading to this isomer have fairly high barriers and tight transition states. This isomer plays only a very minor role in the reaction of CH with C_2H_2.

The two remaining C_3H_3 isomers, 2-propene-1-yl-3-ylidene and 1-propene-1-yl-3-ylidene, are less well defined. The calculated energy barrier (after ZPE correction) for isomerization of 2-propene-1-yl-3-ylidene to 2-propynyl, TS 3, is 0.4 kcal/mol *below* 2-propene-1-yl-3-ylidene itself, indicating a very flat potential energy surface. It is even conceivable that this isomer is no more than a shoulder on the 2-propynyl energy well. The ease with which 2-propynyl and 2-propene-1-yl-3-ylidene radicals interconvert makes inclusion of this latter isomer into the kinetic model necessary, despite its high relative energy of 47 kcal/mol above 2-propynyl, since it will increase the apparent density of states for 2-propynyl. This increase in density of states by either acting as a transient reservoir species or as an anharmonicity contribution, depending on whether TS 3 exists in reality or not, cannot be quantified accurately at the moment; we included 2-propene-1-yl-3-ylidene as a separate species so we can at least capture a large part of the effect without having to resort to a dubious estimation of the anharmonicity contribution. 1-Propene-1-yl-3-ylidene, finally, has low-energy barriers toward cyclization and hydrogen transfer. Also, this isomer has the highest relative energy of all isomers such that, at the CH + C_2H_2 reactant energy levels, it will have the lowest microcanonical equilibrium abundance. It acts primarily as an intermediary structure in the isomerization and could have been removed from the mechanism without much effect but was retained in the kinetic calculations to avoid ambiguity in the treatment of the chain addition entrance channel in the initial reaction (see higher).

The isomerization transition states interconnecting these six isomers (TS 1 through TS 8) are all clearly defined saddle points on the DFT potential energy surface, with some reservations for TS 3 as discussed higher. The single-point CASPT2 relative energies are all very close to the DFT values, with an average deviation of 1 kcal/mol, indicating that the DFT results are reliable estimates for the transition states, so the DFT characteristics were used without modification.

Numerous dissociation pathways were calculated, many of which are barrierless dissociations. As for the isomerization transition states, we used the dissociation transition states that represent a barrier on the PES (TS 9, TS 14, TS 15) without further modification. The barrierless dissociation pathways require a more involved microvariational approach to accurately locate the energy-dependent bottleneck to reaction; the general approach has been discussed earlier. For the dissociation pathways TS 10 through TS13, it was found that the relative energy of the dissociated fragments as a function of the C−H bond length did not converge to the correct limit calculated for the two completely separated fragments. As argued in ref 8,

this nonconvergence is caused by an inaccurate DFT energy for the isolated H atom, deviating from the exact solution of 0.5 hartree. Even though the error is small at the relevant bond lengths (of the order of a few kcal/mol), we choose to correct for it in an approximate manner. In view of the cause of the problem, we can assume that the error is nonexistent for the adduct and exponentially approaching a maximal deviation asymptote at infinite separation. Since this maximal deviation is unknown, we use a truncated exponential as a correcting function, where the energy E_{max} of the geometry with longest C−H bond considered (r_{max}) is corrected so as to correspond to the correct energy limit E_{limit}:

$$E_r^{corr} = E_r - (E_{max} - E_{limit})\frac{1 - \exp(r_{adduct} - r)}{1 - \exp(r_{adduct} - r_{max})}$$

where r is the C−H bond length (in Å), r_{adduct} the equilibrium C−H bond length, and E_r the ZPE-corrected DFT energy. The bond length at which the sum of states is found to be a minimum depends slightly on the precise form of the correcting function used, but the effect on the value of the minimized sum of states is negligible compared to other possible errors. Furthermore, the correction is nearly the same for all barrierless exit channels, such that the relative rates of the different exit channels will hardly be affected.

A comparable problem exists for the initial reaction: the energy of $CH + C_2H_2$ relative to 2-propynyl was calculated at 118 kcal/mol at the DFT level, whereas the CASPT2 energy was 109 kcal/mol; this is probably related to an inaccurate DFT energy for the small CH radical. We opt here to use the thermochemical value of 112 kcal/mol;[8] the energy profile for the initial reaction was corrected using a truncated exponential function identical to that used for adjusting for the $C_3H_2 + H$ dissociation reaction energy profiles.

An issue that was left unresolved in our earlier theoretical paper[8] was the possibility of H_2 elimination from the cyclic C_3H_3 isomers, leading to cyc-$C_3H + H_2$, i.e., a dissociation pathway comparable to the H_2 elimination from linear C_3H_3, which leads to lin-$C_3H + H_2$ with a barrier of 7.5 kcal/mol. Cyc-C_3H and lin-C_3H have nearly the same ground-state energies, but no transition states could be found for the formation of cyc-$C_3H + H_2$. Since then, Kiefer et al.[26] described a transition state with an energy barrier of 32.3 kcal/mol for the dissociation of cyc-C_3H_4 to $C_3H_2 + H_2$, which is comparable to the dissociation of cycloprop-1-enyl to cyc-$C_3H + H_2$. In the assumption that for cycloprop-1-enyl the barrier height is comparably high, this reaction is expected to be unimportant. H_2 elimination from cycloprop-2-enyl is geometrically virtually impossible such that it is reasonable to neglect formation of cyc-$C_3H + H_2$.

Formulation and Solution of the Master Equation

The energy grained Master Equation was constructed using an energy band size of 0.239 kcal/mol (1 kJ/mol), and an energy ceiling of 191.2 kcal/mol (800 kJ/mol) above 2-propynyl. This grid ensures that the energy-specific populations are described with sufficient detail to describe the effects of temperature and pressure changes, with a negligible truncation of the high-energy tail at all temperatures considered. The steady-state approach for the populations of the $C_3H_3^\dagger$ intermediates is valid, since the lifetimes of the activated C_3H_3 intermediates (on the order of nanoseconds) is several orders of magnitude shorter than the time needed to significantly change the concentrations of the reactants C_2H_2 or CH (on the order of milliseconds in flames). Molecules with an internal energy that is at least 9.5 kcal/mol (40 kJ/mol) too small to reach the lowest accessible transition state are collected in a sink; they represent stabilized C_3H_3 radicals and will assume a thermal Maxwell−Boltzman distribution. The unstable 1-propene-1-yl-3-ylidene and 2-propene-1-yl-3-ylidene are never collected in a sink, since the lowest accessible transition state allows for rapid thermal reaction even at the lowest temperature. Cycloprop-1-enyl isomers can easily clear the barriers for isomerization by thermal excitation, except at the lowest temperatures considered (∼100 K). The choice of the sink energy cutoff ensures that the cycloprop-1-enyl sink only collects molecules at or very close to the ground state energy; this effectively collects slow-reacting stabilized molecules at the lowest temperatures, while still allowing thermal isomerization at higher temperatures where only a very small fraction of the thermal distribution occupies the lowest energy grains. The relative abundance of cycloprop-1-enyl isomers with respect to the total amount of C_3H_3, both stabilized and energized, is negligible (≪1%) in all reaction conditions considered; use of the sink here is mainly to avoid numerical overflow errors.

Throughout the calculations, air is used as the bath gas, using literature values[27] for the collision parameters (N_2: $m_r = 28$; $\sigma_{AA} = 3.681$ Å, $\epsilon_{AA} = 91.5$ K; O_2: $m_r = 32$; $\sigma_{AA} = 3.433$ Å, $\epsilon_{AA} = 113$ K). To the best of our knowledge, the collision parameters for C_3H_3 ($m_r = 39$) have not been determined yet; we use estimated[27] values of $\sigma_{AA} = 4.5$ Å and $\epsilon_{AA} = 260$ K for all C_3H_3 isomers, with an estimated[28−30] average transferred energy per collision $\langle \Delta E_{all} \rangle = -0.48$ kcal/mol (-168 cm^{-1}) at the internal energies as formed initially in the initial reaction. The value for $\langle \Delta E_{all} \rangle$ will be too high at smaller internal energies, but since thermal re-energization up to the dissociation pathways is unlikely, this will not influence the calculated stabilization rate.

Despite the size of the mechanism, the small size of the grains, and the high energy ceiling, the steady-state CSSPI method, using a 3431 × 3431 matrix, proved numerically stable for all temperatures and pressures considered, inducing no visual deviations or numerical errors except for some small round-off errors in the least significant digits many orders of magnitude less than the error induced by uncertainties on the input data and theoretical models used. As already mentioned, the CSSPI results were verified against DCPD[10] calculations. Despite the large matrix sizes (3440 × 3440 elements for the DCPD) and the difference in matrix setup, matrix conditioning, and numerical solution algorithm, the results of both methods agree in (at least) the eight most significant digits for all calculations performed, indicating that both methods are numerically very stable and that neither induces a significant error in the calculated product distribution.

Error Analysis

To assess the accuracy of the calculated product distribution with respect to the input parameters in the theoretical kinetical model, we performed an error analysis based on a brute force approach, where several parameters in the kinetic model were varied and the resulting shift in the pressure- and temperature-dependent product distribution was calculated. Each parameter considered was varied twice, once to each extreme of its confidence interval; this leads directly to a pressure- and temperature-dependent confidence interval for the predicted product distribution corresponding to the actual *impact* of the uncertainty of the considered parameter. As a result of the enormous volume of data generated, it is impossible to give

here a detailed account for each parameter. In the discussion below, we will therefore refer to an overall error, obtained by error propagation of the individual errors: $\sigma_{overall} = (\sum \sigma_i^2)^{1/2}$. The confidence intervals on the product distribution are in general asymmetric; we always use the largest half of the interval as σ_i in the calculation of the overall error such that the error is never underestimated.

Varying every single parameter in the model (wavenumbers, relative energies,...) would make the error analysis unwieldy and computationally very expensive. Also, this overly detailed approach would make the interpretation of the results difficult, since the errors on many of the parameters (e.g., wavenumbers) are unknown and tend to have the same effect on the product distribution as other parameters. To keep the number of variations down to an acceptable level, we opted for varying groups of parameters rather than individual parameters, chosen such that specific and important aspects in the kinetic model are addressed. For example, varying the $C_3H_2 + H$ dissociation energy models not only the uncertainty on those relative energies but also other properties that enhance or reduce the rate of dissociation to $C_3H_2 + H$, such as the energy profile used for the microvariational TS, anharmonicity effects in the TS or adducts, centrifugal effects, etc. Two scenarios were considered: one based on the estimated uncertainties on the parameters and a worst-case scenario based on an estimated upper limit for the confidence interval.

A first group of parameters varied simultaneously are the isomerization barrier heights. On the basis of the difference between the B3LYP-DFT, the CASPT2, and the available literature data, we estimate the probable error on these barrier heights to be about ±2 kcal/mol, while for the worst-case scenario we use a confidence interval of ±4 kcal/mol. This group of parameters serves as a model for all modifications that affect the rate of isomerization. A second group of parameters is the height of the dissociation limit energy for barrierless pathways to $C_3H_2 + H$, again with an estimated probable error of ±2 kcal/mol (worst case: ±4 kcal/mol). This uncertainty is large enough to account also for errors in the energy profile corrections for the barrierless reactions. Because the correction on the energy profile for the initial reactions was larger than that for the $C_3H_2 + H$ dissociation channels, we postulate an uncertainty of ±3 kcal/mol for the $C_2H_2 + CH$ relative energy (worst case: ±5 kcal/mol), despite our use of the experimental relative energy value. The relative importance of the different entrance channels is varied by 10 percentage points (absolute). To assess any errors in the relative importance of the two major C_3H_3 dissociation channels, i.e., 2-propynyl → HCCCH + H and cycloprop-2-enyl → cyclo-C_3H_2 + H, the relative energies of the two dissociation limits are varied simultaneously but in the opposite sense by ±2 kcal/mol (worst case: ±4 kcal/mol). An important source of error is also the collisional energy transfer model used, in particular the average transferred energy per collision, $\langle \Delta E_{all} \rangle$, on which it relies heavily. Since our value for $\langle \Delta E_{all} \rangle$ is merely estimated based on "comparable" systems, we associate a large error of 50% with it; $\langle \Delta E_{all} \rangle = 0.48 \pm 0.24$ kcal/mol. For the worst-case scenario, we also considered that the density of states of the C_3H_3 adducts could be underestimated because of neglected anharmonicity. The effect of this is estimated by artificially tripling the harmonic densities of states for all the C_3H_3 radicals.

Even though solution methods for the *E*,*J*-specific two-dimensional Master Equation exist,[31,32] the Master Equation as it was formulated above does not include centrifugal effects caused by overall molecular rotation. For the isomerization reactions, the moments of inertia do not change drastically, making inclusion of rotational effects unnecessary. Dissociation of C_3H_3 to $C_3H + H_2$ occurs through fairly tight transition states, again with comparatively small changes in the moments of inertia. The change in moments of inertia for the barrierless dissociations to $C_3H_2 + H$ is also fairly small, since only a light hydrogen atom is ejected. This leaves only the initial reaction and its reverse—with C_3H_3 molecules redissociating into two comparably heavy fragments C_2H_2 and CH—as a reaction where centrifugal effects may be important. However, changing the rate of redissociation will barely affect the calculated *net* product distribution, and the fraction of redissociation is always so small (see below) that the correction to the overall rate constant for the $C_2H_2 + CH$ reaction will be comparable to currently attainable experimental accuracy. Hence, inclusion of centrifugal effects in this system should have a fairly small effect on the calculated product distribution, swamped by the errors due to uncertainties on more sensitive parameters, as described above.

Finally, there is also the possibility of errors due to the inadequacy of the theoretical kinetical models used: nonergodicity at very high internal energies, state-selectivity effects at very low temperatures, deviation from the ideal gas model at high pressures, the collision model itself, etc. The impacts of these possible errors are almost impossible to verify and quantify, especially since there is virtually no experimental data to compare against, but should only become important in the most extreme of reaction conditions, which have limited practical importance.

Results and Discussion

The results of the product distribution analysis are depicted in Figure 2. The estimated error on the product distribution of the principal reaction products is shown in Figure 3, expressed as the absolute deviation in percentage points derived from the error analysis described earlier. For a few selected reaction products, Figure 4 also gives the absolute error (in percentage points) as derived from the worst-case scenario.

The Initial Reaction and Redissocation to the $C_2H_2 + CH$ Reactants. In all reaction conditions considered, redissociation is an exit channel of small to medium importance (≤13%), depending mainly on the temperature. No pressure dependence is obvious at pressures below 100 atm; at higher pressures, a small falloff behavior can be seen, but even at 10^4 atm the high-pressure limit is not yet fully reached for elevated temperatures. The error on the redissociation fraction is not very large (a few percentage points) and is mainly due to the uncertainty in the relative energy of the $C_2H_2 + CH$ fragments. Some effect may also be expected from anharmonic contributions to the density of states for the intermediates, yielding an even smaller redissociation fraction. Given the small redissociation fraction, even at high temperatures, and the absence of a barrier in the entrance channel, the apparent overall rate constant for the $CH + C_2H_2$ reaction will always be close to the collision limit, within chemical accuracy. This agrees with recent experimental measurements[22] (Table 1), which show no apparent pressure dependence at pressures up to 400 Torr. A slight negative temperature dependence as suggested by some of the experimental data[22,25] might be attributable to the variational character of the entrance transition state. Since the overall rate constant has already been well-established experimentally, no attempt was made at this time to study the temperature dependence of the $C_2H_2 + CH$ bimolecular rate constant by detailed microvariational TST calculations. Canonical flexible TST calculations, which include centrifugal effects, yielded rate constants

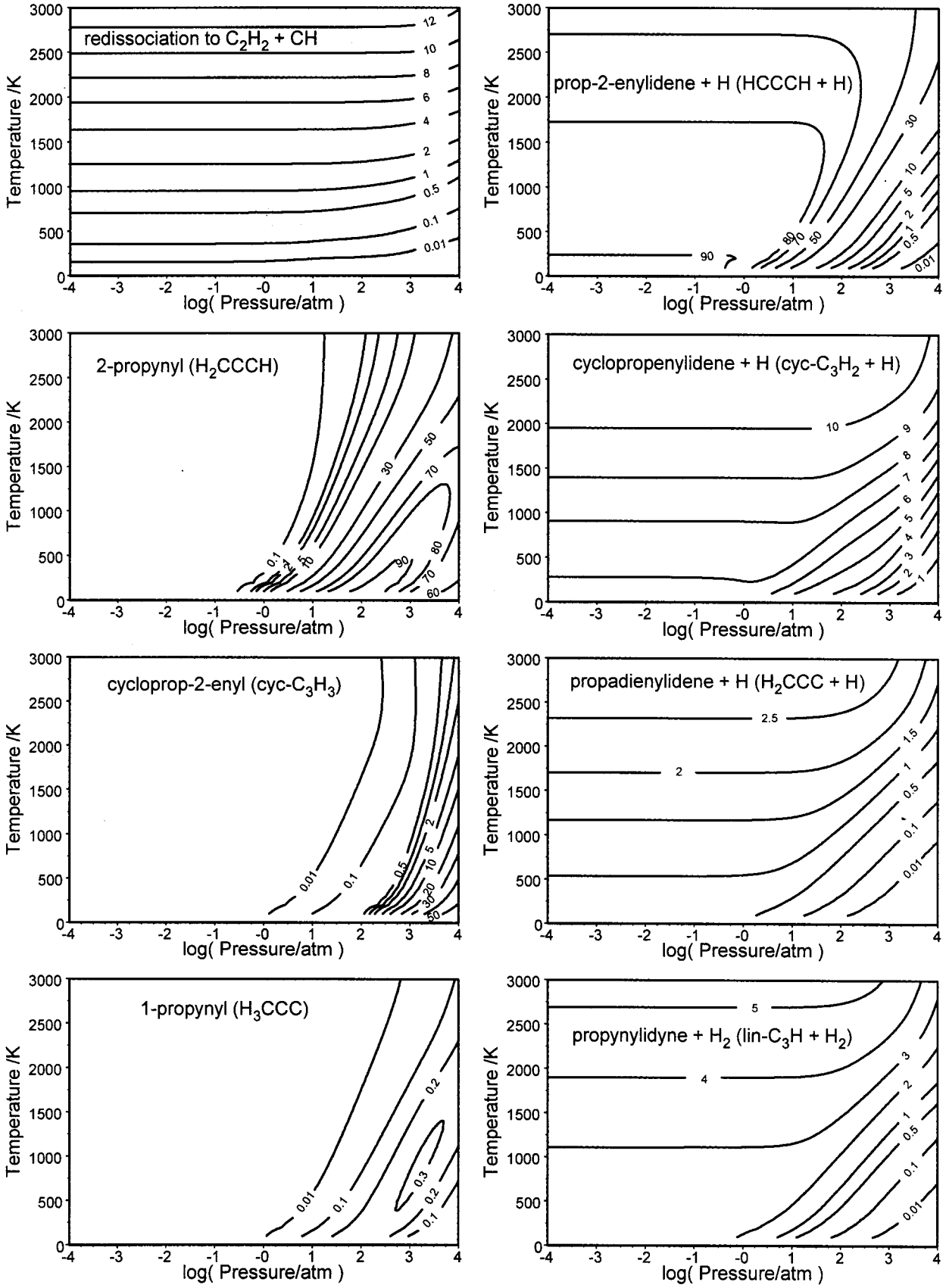

Figure 2. Pressure- and temperature-dependent product distribution (%) for the C_2H_2 + CH($X^2\Pi$) reaction. Some distortion of the contours near 100 K is due to the graphical interpolation.

around 3×10^{-10} cm^3 molec^{-1} s^{-1}, showing little temperature dependence, in accordance with the most recent experimental data[22] and the VTST calculations of Guadagnini et al.[9]

The (lack of) effect of altering the adopted relative contributions of the different entrance channels is also interesting. The resulting changes in the calculated product distribution are

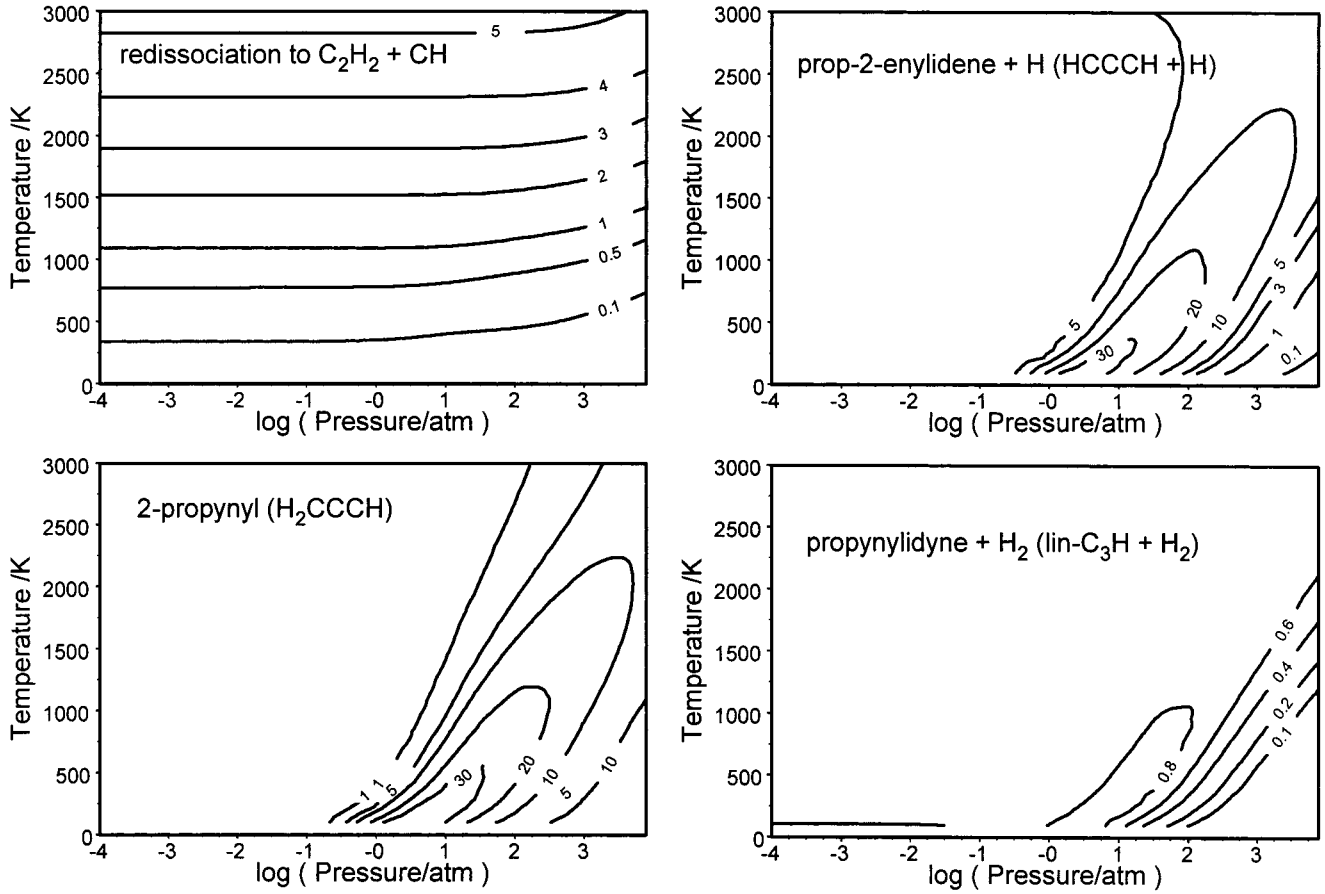

Figure 3. Pressure- and temperature-dependent estimated error in percentage points (absolute) on the product distribution for the principal products.

negligible compared to the other uncertainties. In fact, sample calculations showed that modifying the initial reaction to consist of 100% cycloaddition, 100% insertion, or 100% chain addition does not affect the redissociation fraction or the ratio of stabilization versus dissociation appreciably and only changes the absolute yields of cyclic versus linear reaction products by about 15 percentage points from the values reported here. For example, at 1500 K and 1 atm, we normally find 82% of HCCCH + H and 9% cyc-C_3H_2 + H (Figure 2). Assuming 100% cycloaddition, the yields changes to 75% HCCCH + H and 15% cyc-C_3H_2 + H; for the insertion channel, we find 91% and 2%, while solely chain addition yields 81% and 8%. This leads to the conclusion that interconversion of the various C_3H_3 isomers is sufficiently fast to attenuate the effect of these changes almost completely such that the relative importance of the different entrance channels becomes a minor issue. The fast isomerization is also supported by the error analysis, where altering the isomerization barrier height has only a moderate effect on the calculated product distribution.

Falloff Behavior: Dissociation versus Stabilization. Despite the lack of a clear falloff behavior for the overall rate constant, two distinct pressure regimes can be distinguished for the product distribution, separated by a transition region. In the high-pressure regime, the products are stabilized C_3H_3 isomers, whereas in the low-pressure regime, stabilization is absent and C_3H_2 + H and C_3H + H_2 are the main reaction products. Predicting the position of the transition region, separating the low-pressure and high-pressure regimes, is currently the Achilles' heel of all Master Equation analyses: it depends strongly on the energy transfer characteristics of the intermediates and the bath gas, for which there is usually little data available. While the functional form of the energy transfer probabilities is relatively well understood[28−30] and appropriately described by models such as the biexponential model of Troe, the parameters to be used in these models can often only be estimated. Also, there are other factors here that can influence the positioning of the falloff, such as anharmonicity effects and the relative energy of the C_3H_x + H_y dissociation limit with respect to the energy of the C_2H_2 + CH reactants. It is therefore not surprising that the largest predicted errors on the product distribution are found precisely for the midpoint of the transition region, located around 10 atm at 100 K and 1000 atm at 2000 K. The error analysis includes the most sensitive parameters, with important contributions from the uncertainty on the energy transferred per collision, $\langle\Delta E_{all}\rangle$, and the energy of C_2H_2 + CH relative to the most important dissociation channels (formation of HCCCH + H and cyc-C_3H_2 + H). The effect of possible anharmonicity contributions for the C_3H_3 intermediates, increasing the density of states and therefore the lifetime, was also verified in the worst-case error analysis scenario. From these detailed calculations, we conclude that there can be an error of about an order of magnitude in pressure on the location of the transition regime. Because of the comparatively abrupt changes of the product distribution as a function of the pressure in this regime, care must be taken when using the predicted product distribution for these temperature and pressure combinations. Note that most of the uncertainty could be removed if some experimental product distribution measurements were available in this regime, permitting calibration of the model.

Most real-world applications where the CH + C_2H_2 reaction is important are in the low-pressure regime. Examples are combustion processes at pressures near or below atmospheric, experimental flow tube and shock tube setups for studying combustion systems, and interstellar chemistry. According to

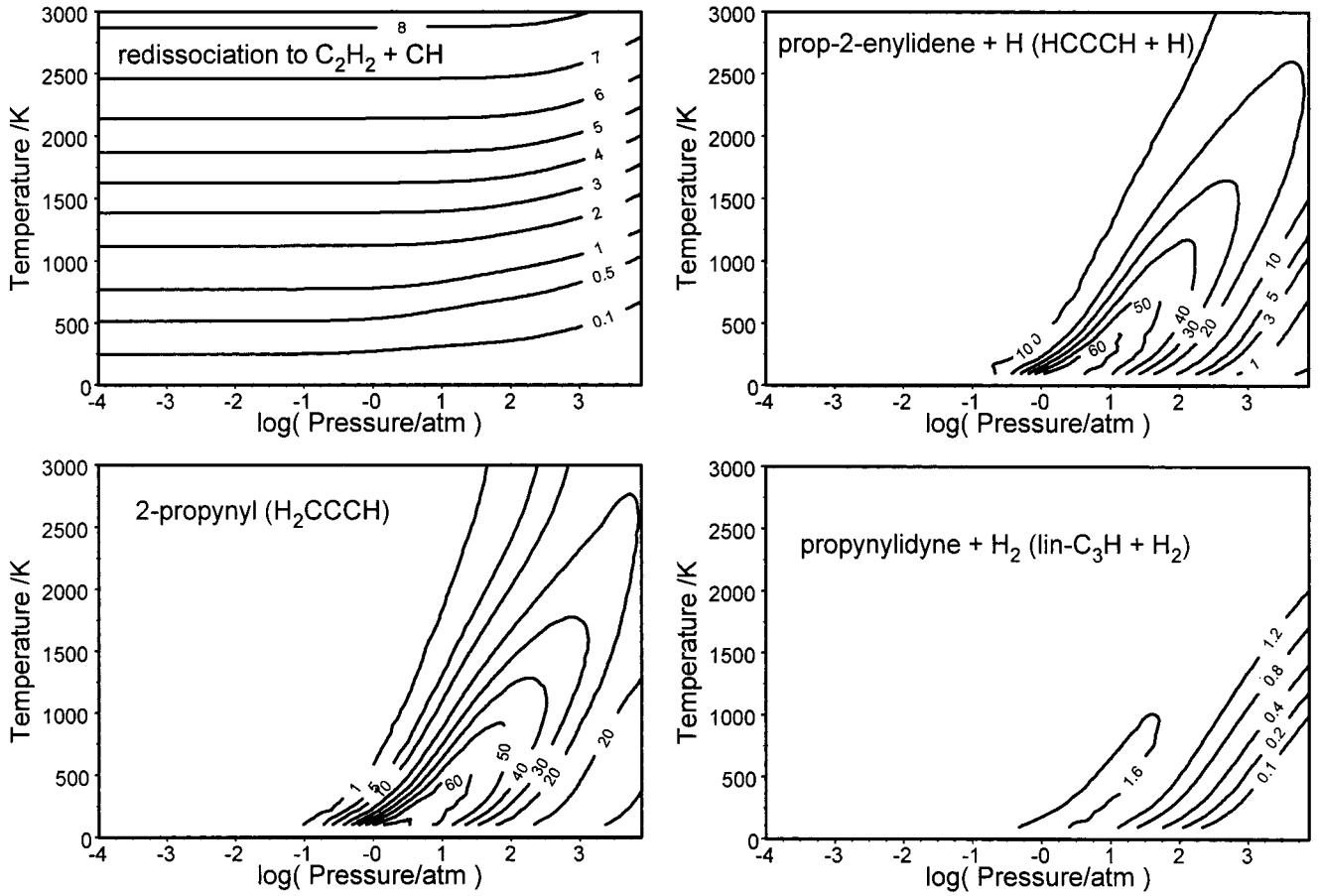

Figure 4. Pressure- and temperature-dependent estimated error in percentage points (absolute) on the product distribution for the principal products, based on a worst-case scenario.

our findings, stabilization of C_3H_3 is negligible for these systems while the dissociation routes to C_3H_2 + H and C_3H + H_2 are the most important reaction channels (see below).

Stabilization of C_3H_3 Adducts. 2-Propynyl (H_2CCCH) is by far the most stable C_3H_3 isomer, and all C_3H_3 intermediates are initially formed with sufficient energy to clear the isomerization energy barriers. Hence, propargyl is always the intermediate with the highest relative abundance and is the main stabilization product at elevated pressures, unless the pressure is so high that the rate of collisional stabilization exceeds even the rapid isomerization rates. This can be clearly seen in Figure 2, showing that 2-propynyl becomes an increasingly more important product as the pressure increases (above 1 atm). At low temperatures and extremely high pressures, a maximum in the propargyl yield can be seen, beyond which collisional de-energization is faster than isomerization such that the C_3H_3 radicals are no longer in quasi-steady state but retain the same relative importance as dictated by the contributions of the three initial reaction channels. Only for these extreme reaction conditions, which are mainly of academic interest, can other C_3H_3 radicals such as cycloprop-2-enyl become important reaction products. The error in the relative yield of the different C_3H_3 radicals under these conditions is determined by the uncertainty on the relative importance of the different entrance channels and the uncertainty on the relative densities of states for the intermediates.

The isomerization transition state barriers for the chain addition adduct, 1-propene-1-yl-3-ylidene, are too low for this radical to have any significant probability of stabilization. It will always isomerize to 2-propynyl or cycloprop-2-enyl. Its relative concentration is always very small compared to that of the two most stable C_3H_3 isomers. Likewise, the barriers to isomerization for cycloprop-1-enyl are very low, and (thermal) isomerization to 2-propynyl will be its main fate. Even at the lowest temperature considered, 100 K, no significant stabilization of cycloprop-1-enyl was ever found. For 1-propynyl, a very small yield ($\leq$0.3%) was found in a narrow window corresponding to the transition region. This is related to the fact that 1-propynyl is only accessible through two fairly high isomerization barriers; it can only be formed if dissociation to C_3H_2 + H is already hampered by collisional de-energisation, but stabilization of the C_3H_3 intermediates remains sufficiently slow to allow for some isomerization to 1-propynyl.

As discussed earlier, 2-propene-1-yl-3-ylidene was mainly incorporated to include part of the anharmonicity correction for 2-propynyl. The interconversion of these two intermediates is very fast, ensuring partial microcanonical equilibrium at all times. As a result, the relative abundance of the 2-propene-1-yl-3-ylidene is fairly high, i.e., a few percent of that of 2-propynyl.

Dissociation of the C_3H_3 Species to C_3H_2 + H and to C_3H + H_2. For the low-pressure regime, the main fate of the intermediates is dissociation. Formation of triplet prop-2-ynylidene (HCCCH) is by far the most important dissociation channel, with yields up to 90% for low-pressure, low-temperature reaction conditions. Several factors contribute to this. The HCCCH + H exit channel is directly accessible from 2-propynyl, which has the highest abundance of the intermediate C_3H_3 species. Also, HCCCH is a rather loose molecule, and consequently has a very high density of states such that the sum of states $G^{\ddagger}(E - E_0)$ for the barrierless, *product-like* dissociation transition state is high compared to the other dissociation

channels. Combining this with the fact that it is energetically the second most favorable exit channel makes dissocation to prop-2-ynylidene the most important reaction channel. The lowest accessible exit channel, leading to the formation of cyclopropenylidene + H, is also a barrierless reaction, but the rigid three-membered ring has fairly high vibrational wavenumbers such that this channel has a comparatively lower sum of states. Also, the relative steady-state abundance of its parent adduct, cycloprop-2-enyl, is always significantly lower than that of propargyl. Because of the stronger energy dependence of the sum of states for this transition state compared to that of the HCCCH + H dissociation channel, the contribution of the former dissociation channel increases at higher temperatures, with the cyc-C_3H_2 yield reaching a maximum contribution of 11% at the highest considered temperature of 3000 K. The calculated yields of cyc-C_3H_2 + H should be considered as lower limits, since they are fairly dependent on the relative concentration of the cyc-C_3H_3 concentration, which in turn depends on the relative density of states of cyc-C_3H_3 compared to 2-propynyl. Because of the highly flexible nature of excited cycloprop-2-enyl, its density of states and that of the transition state TS 13 are probably underestimated, indicating that the true abundance of cyc-C_3H_3 and the yield of cyc-C_3H_2 + H are probably higher. Dissociation of cycloprop-1-enyl to cyc-C_3H_2 + H is less important because of the presence of a barrier to dissociation and the very low abundance of cycloprop-1-enyl. The third dissociation channel in the mechanism, 2-propynyl → H_2CCC + H, is a fairly minor channel, and the H_2CCC yield never reaches more than 3% even at the highest temperature of 3000 K. Obviously, this can be explained by the higher relative energy and the somewhat tighter transition state (compared to that for dissociation to HCCCH + H) such that this exit channel only comes into play at higher temperatures. While there are C_3H_2 + H dissociation products possible other than those included in our PES,[8] they all have even higher relative energies and will therefore have even smaller contribution. The errors calculated on the relative contributions for each of the C_3H_2 + H channels are mainly a function of the uncertainties on the dissociation limits, allowing for a shift in the HCCCH/cyc-C_3H_2 yields of about 3−5 percentage points (absolute).

The lowest transition state for the formation of lin-C_3H + H_2, TS 14, has an energy barrier comparable to the HCCCH + H dissociation limit. Formation of HCCC + H_2 was found to be much less important, with a maximum calculated yield of about 5% at 3000 K. Formation of HCCC + H_2, from 2-propynyl, must compete with the dissociation of C_3H_3 to C_3H_2 + H. Because C_3H_2 + H formation occurs mainly through barrierless transition states, with rate constants that must be minimized in a microvariational approach, it is conceivable that the C_3H + H_2 yield could actually be higher, since increasingly rigorous treatment of the C_3H_2 + H formation tends to decrease the minimized rate constants. Also, the height of the H_2 elimination barrier relative to the HCCCH + H dissociation limit will influence the C_3H_2/C_3H product ratio.

Boullart et al.[7] determined the product distribution of the CH + C_2H_2 reaction experimentally at 600 K and 2 Torr, finding yields of 85^{+9}_{-15}% C_3H_2 + H and 15^{+15}_{-9}% C_3H + H_2, i.e., a somewhat higher C_3H + H_2 yield then found in our calculations.

Comparison with Another RRKM Study. To our knowledge, only one other RRKM study of the CH + C_2H_2 reaction has been published, providing the only theoretical product distribution data available for comparison. This very recent study by Guadagnini et al.[9] is intended for use in zero-pressure or low-pressure conditions, lacking a Master Equation analysis to account for collisional energy transfer processes at higher pressures. Barrierless reactions are described based on a variational approximation using interpolated vibrational characteristics between reactant and products, as opposed to our full microvariational treatment employing a detailed quantum chemical characterization of energies and vibrational frequencies along the reaction coordinate.

While both our and their studies concur that redissociation is a minor channel, this is as far as the agreement goes. Guadagnini et al. find that H_2CCC + H is the main product, with a negligible amount of HCCCH + H and no possibility for formation of cyc-C_3H_2 + H. This result is almost the opposite of our findings, where H_2CCC + H is only a minor channel. The discrepancy can be attributed entirely to the potential energy surface used, which is highly incomplete in the case of ref 9. Dissociation of 2-propynyl is only allowed to H_2CCC + H, ignoring the energetically and entropically more favorable barrierless dissociation to H + HCCCH (called "cyclic" in ref 9 despite its near linearity), which in their PES can only be formed through a very high and tight transition state starting from 1-propene-1-yl-3-ylidene. Moreover, the PES used in ref 9 neglects isomerization to cyclic C_3H_3 isomers, taking into account only 2-propynyl and the two highest lying isomers, 1-propene-1-yl-3-ylidene (3 internal rotameric forms) and 2-propene-1-yl-3-ylidene. Obviously, this also prohibits inclusion of the energetically most favorable exit channel to cyc-C_3H_2 + H. No C_3H + H_2 formation was considered. Finally, and of minor importance, in ref 9, the initial reaction is described solely in terms of the radical chain addition, despite that the carbyne character of CH is well-documented and that carbyne + closed-shell reactions, leading to cycloaddition and insertion, are in general much faster than radical + closed-shell reaction pathways. The crucial role of the carbyne character of CH in the reaction with closed-shell species can be illustrated[33−36] by the difference in reaction rates of CH and CF with various types of reactants. That the neglect of the carbyne entrance channels in ref 9 is of less importance here is owed to the fast interconversion of the C_3H_3 intermediates. While the PES used in our study might also ommit certain aspects or contain inaccuracies, it was thoroughly checked against available literature data,[8] not revealing any significant errors or gaps in our quantum chemical characterization. We feel that the PES as characterized by us[8] includes the most important elementary reactions one expects based on the general chemical properties of the pertaining reactants and intermediates, providing a reliable basis for an RRKM analysis of this system.

Conclusions

The product distribution for the CH($X^2\Pi$) + C_2H_2 reaction has been investigated theoretically over extended temperature and pressure ranges, based on a microvariational RRKM approach combined with Master Equation analysis. In a low-pressure region, covering most practical reaction systems where the title reaction is important, the main fate of the C_3H_3 intermediates is dissociation to HCCCH + H and cyc-C_3H_2 + H, with smaller fractions dissociating to C_3H + H_2 and redissociating to C_2H_2 + CH. Because most exit channels are fast, barrierless dissociation reactions with product levels up to 25 kcal/mol below the reactant energy level, high pressures in excess of 10−100 atm of air are needed to stabilize the intermediary C_3H_3 radicals, with propargyl (H_2CCCH) being the primary product in the high-pressure limit. In all reaction conditions examined, redissociation to C_2H_2 + CH remains a minor process.

To assess the uncertainties in these results, an error analysis was performed on the product distribution calculations, by varying all important parameters in the kinetic model. As expected, the largest errors are found for the ratio of dissociation versus stabilization in the transition region between low- and high-pressure regimes; an uncertainty of 1 order of magnitude in pressure is found for the center of the transition region. The precise relative importance of the different entrance channels was found to be of minor importance for the product distribution because of fast isomerization of the activated C_3H_3 intermediates. The uncertainties in the contributions of the other product channels are not overly large, having no significant impact on the basic conclusions. The ratio of the C_3H_2 + H versus C_3H + H_2 yields and the ratio of HCCCH/cyc-C_3H_2 product formation could be affected by anharmonic effects that were not included here in the calculation of the densities of states for the intermediates and the sum of states of the transition states.

Acknowledgment. The support from the European Commission and the Fonds voor Wetenschappelijk Onderzoek, Belgium is gratefully acknowledged.

References and Notes

(1) Wu, C.; Kern, R. *J. Chem. Phys.* **1987**, *91*, 6291.
(2) Kern, R. D.; Wu, C. H.; Yong, J. N.; Pamidimukkala, K. M.; Singh, H. J. *Energy Fuels* **1988**, *2*, 454.
(3) Peeters, J.; Boullart, W.; Devriendt, K. *J. Phys. Chem.* **1995**, *99*, 3583.
(4) Peeters, J. *Bull. Soc. Chim. Belg.* **1997**, *106*, 337.
(5) Abramovich, R. A., Ed. *Reactive Intermediates*; Plenum: New York, 1980. Almond, M. J., Ed. *Short-Lived Molecules*; Ellis Horwood: New York, 1990. Matthews, H.; Irvine, W. M. *Apstrophys. J.* **1985**, *298*, L61. Thaddeus, P.; Vrtilek, J. M.; Gottlieb, C. A. *Astrophys. J.* **1985**, *299*, L63; Cernicharo, J.; Gottlieb, C. A.; Guélin, M.; Killian, T. C.; Paubert, G.; Thaddeus, P.; Vrtilek, J. M. *Astrophys. J.* **1991**, *368*, L39.
(6) Kaiser, R. I.; Ochsenfeld, C.; Stranges, D.; Head-Gordon, M.; Lee, Y. T. *Faraday Discuss.* **1998**, *109*, 183.
(7) Boullart, W.; Devriendt, K.; Borms, R.; Peeters, J. *J. Phys. Chem.* **1996**, *100*, 998.
(8) Vereecken, L.; Pierloot, K.; Peeters, J. *J. Chem. Phys.* **1998**, *108*, 1068.
(9) Guadagnini, R.; Schatz, G. C.; Walch, S. D. *J. Phys. Chem. A* **1998**, *102*, 5866.
(10) Vereecken, L.; Huyberechts, G.; Peeters, J. *J. Chem. Phys.* **1997**, *106*, 6564.
(11) Robinson, P.; Holbrook, K. *Unimolecular Reactions*; Wiley-Interscience: London, 1972.
(12) Forst, W. *Theory of Unimolecular Reactions*; Academic Press: New York; 1973.
(13) Gilbert, R.; Smith, S. C. *Theory of Unimolecular and Recombination Reactions*; Blackwell Scientific: Oxford; 1990.
(14) Holbrook, K.; Pilling, M.; Robertson, S. *Unimolecular Reactions*, 2nd ed.; Wiley: New York; 1996.
(15) Beyer, T.; Swinehart, D. F. *Comm. Assoc. Comput. Machines* **1973**, *16*, 379.
(16) Stein, S. E.; Rabinovitch, B. S. *J. Phys. Chem.* **1973**, *58*, 2438.
(17) Klippenstein, S. J. *J. Phys. Chem.* **1991**, *94*, 6469.
(18) Klippenstein, S. J. *J. Phys. Chem.* **1994**, *98*, 11459.
(19) Smith, S. C. *J. Phys. Chem.* **1993**, *97*, 7034.
(20) Wardlaw, D. M.; Marcus, R. A. *J. Chem. Phys.* **1985**, *83*, 3462.
(21) Troe, J. *J. Chem. Phys.* **1977**, *66*, 4745, 4758.
(22) Thiesemann, H.; MacNamara, J.; Taatjes, C. A. *J. Phys. Chem. A* **1997**, *101*, 1881.
(23) Bosnali, M. W.; Perner, D. *Z. Naturforsch.* **1971**, *26A*, 1768.
(24) Butler, J. E.; Fleming, J. W.; Goss, L. P.; Lin. M. C. *Chem. Phys.* **1981**, *56*, 355.
(25) Berman, M. R.; Fleming, J. W.; Harvey, A. B. *Chem. Phys.* **1982**, *73*, 27.
(26) Kiefer, J. H.; Mudipalli, P. S.; Sidhu, S. S.; Kern, R. D.; Jursic, B. S.; Xie, K.; Chen, H. *J. Phys. Chem. A* **1997**, *101*, 4057.
(27) Hirschfelder, J. O.; Curtiss, C. F.; Bird, R. B. *Molecular Theory of Gases and Liquids*; John Wiley & Sons: New York, 1967.
(28) Tardy, D. C.; Rabinovitch, B. S. *Chem. Rev.* **1977**, *77*, 369.
(29) Oref, I.; Tardy, D. C. *Chem. Rev.* **1990**, *90*, 1407.
(30) Flynn, G. W.; Parmenter, C. S.; Wodtke, A. M. *J. Phys. Chem.* **1996**, *100*, 12817.
(31) Jeffrey, S. J.; Gates, K. E.; Smith, S. C. *J. Phys. Chem.* **1996**, *100*, 7090.
(32) Diau, E. W.-G.; Smith, S. C. *J. Phys. Chem.* **1996**, *100*, 12349
(33) Peeters, J.; Van Hoeymissen, J.; Vanhaelemeersch, S.; Vermeylen, D. *J. Phys. Chem.* **1992**, *96*, 1257.
(34) Van Hoeymissen, J.; De Boelpaep, I.; Uten, W.; Peeters, J. *J. Phys. Chem.* **1994**, *98*, 3725.
(35) De Boelpaep, I.; Vetters, B.; Peeters, J. *J. Phys. Chem. A* **1997**, *101*, 787.
(36) James, F. C.; Choi, H. K.; Ruzsicska, B.; Strausz, O. P. *Frontiers of Free Radical Chemistry*; Pryor, W. A., Ed.; Academic Press: New York, 1980; p 139.